Synthesis and Characterization of Network Type Single Ion Conductors

Xiao-Guang Sun, Craig L. Reeder, and John B. Kerr*

Lawrence Berkeley National Laboratory, MS 62-203, One Cyclotron Road, Berkeley, California 94720

Received November 10, 2003; Revised Manuscript Received January 9, 2004

ABSTRACT: New single ion conductors were synthesized by grafting the allyl group-containing lithium salt, lithium bis(allylmalonato)borate (LiBAMB), onto allyl group-containing comb-branch polyacrylate or polymethacrylate ethers by means of hydrosilylation. The highest ambient temperature conductivity of 3.5×10^{-7} S cm^{-1} was obtained for a polyacrylate ether-based single ion conductor containing eight EO units in the side chain and five EO units in the cross-linking side chain, to which the anion was fixed with a salt concentration of EO/Li = 20. For polyacrylate ether-based single ion conductors, an increase of chain length in both side chains and cross-linking anion chains favors an increase of ionic conductivity. The addition of 50 wt % EC/DMC (1/1, wt/wt) increased the ionic conductivity by more than 2 orders of magnitude due to both the increase in ionic mobility from the liquid phase and the increase in the concentration of free ions from the high dielectric constant of the solvent. The preliminary Li/Li cycling profiles of dry polyacrylate- and polymethacrylate ether-based single ion conductors are encouraging as almost no concentration polarization or relaxation was observed. The observed increase in cell potential with cycling is apparently due to an increase in the interfacial impedance associated with the SEI layer, and the cell failure is accompanied by the decomposition of the ester bond of the polyacrylate backbone.

1. Introduction

Conventional solid polymer electrolytes are formed by the dissolution of salts in a suitable polymer host, and thus both cation and anion are mobile.[1] However, since lithium batteries only involve the intercalation/deintercalation and plating/stripping of the lithium cations, practical cells using these conventional binary salt electrolytes will suffer from problems caused by concentration gradients of the salt and cell polarization, which eventually results in battery failure. Therefore, in practical applications, polymer electrolytes with high Li^+ transference numbers are highly preferred. So far, there are two approaches of increasing Li^+ ion transference number in polymer electrolytes. One is to incorporate electronically deficient moieties into the polymer chain, which can act as an anion-trapping site to limit the free movement of anions.[2,3] In this system, a Li^+ transference number as high as 0.7 has been realized. Another approach is to chemically attach the anions to the polymer backbones, so that Li^+ transference number of one, a single ion conductor, can be realized.[4−12] Most of the single ion conductors have been synthesized by fixing either alkyl sulfonate[4,5] or carboxylate[6,7] to the polymer backbone. However, the ion dissociation in polyether media is very limited, and as a result, the ambient temperature conductivities are very low, usually in the range 10^{-8}−10^{-7} S cm^{-1}. To enhance the ionic dissociation and improve room temperature ionic conductivity, polyelectrolytes with different anions have been synthesized,[8−12] and the resulting conductivities have increased to the range 10^{-7}−10^{-5} S cm^{-1}. Among them, higher ionic conductivities are usually found for oligomers, low molecular weight polymers with poor mechanical properties, so they cannot be used for commercial devices where thin films are preferred. The synthesis of single ion conductors with both high ambient conductivity and high mechanical strength presents a challenge.

* Corresponding author: e-mail jbkerr@lbl.gov; Tel 1-510-486-6279; Fax 1-510-486-4995.

In this paper we report the synthesis of a new lithium salt, lithium bis(allylmalonato)borate (LiBAMB), and its incorporation into polymers to form single ion conductors. Synthesis of this new salt is based on two considerations. One is that the new salt (LiBAMB) is similar to the recently studied lithium bis(oxalato)borate (LiBOB)[13] in which the lithium cation is well dissociated from the anion. It is expected that the new salt should be well dissociated in the polymer media so that higher conductivities can be obtained. The other consideration is that LiBAMB has allyl groups on both sides, and after attachment to the polymer through tetramethyldisiloxane by means of hydrosilylation, it not only acts as a lithium source but also acts as a cross-linking site to enhance the mechanical properties of the resulting single ion conductors. So far, examples of papers using lithium salts both as the lithium source and the cross-linker are rare.[8,10] In this paper the synthesis, characterization, and Li/Li cell performance of these new network single ion conductors are reported.

2. Experimental Section

2.1. Materials. Allyloxyethanol, 2-[2-chloroethoxy]ethanol, 3,4-dihydro-2*H*-pyran, acrylic acid, methacrylic acid, tetrabutylamonium hydrogen sulfate, triethylene glycol monomethyl ether, polyethylene glycol monomethyl ether acrylate (M_n = 454, n = 8), polyethylene glycol monomethyl ether methacrylate (M_n = 475, n = 8), hydrochloric acid, diethyl malonate, trimethyl borate, allyl bromide, trichloromethylsilane, 1,2-dichloroethane, 1,1,3,3-tetramethyldisiloxane, sodium metal, lithium ribbon, toluene, benzene, anhydrous methanol, anhydrous ethanol, anhydrous $MgSO_4$, NaOH pellet, and KOH pellet were all obtained from Sigma-Aldrich and were used directly without further purification. Tetrahydrafuran (B&J, distilled in glass) was obtained from VWR and was refluxed over CaH_2 for several days before use. AIBN was recrystallized from methanol twice. The platinum−divinyltetramethyldisiloxane complex in vinylsilicon was obtained from Gelest, Inc.

2.2. Synthesis of Monomers (Scheme 1). *2-[2-(2-Chloroethoxy)ethoxy]tetrahydropyran* was synthesized from the addition of 2-(2-chloroethoxy)ethanol to 3,4-dihydro-2*H*-pyran with hydrochloric acid as catalyst. The crude addition product was dissolved in ether and neutralized with dilute NaOH

10.1021/ma035690g CCC: $27.50
Published on Web 02/26/2004

Scheme 1. Synthesis of Monomers

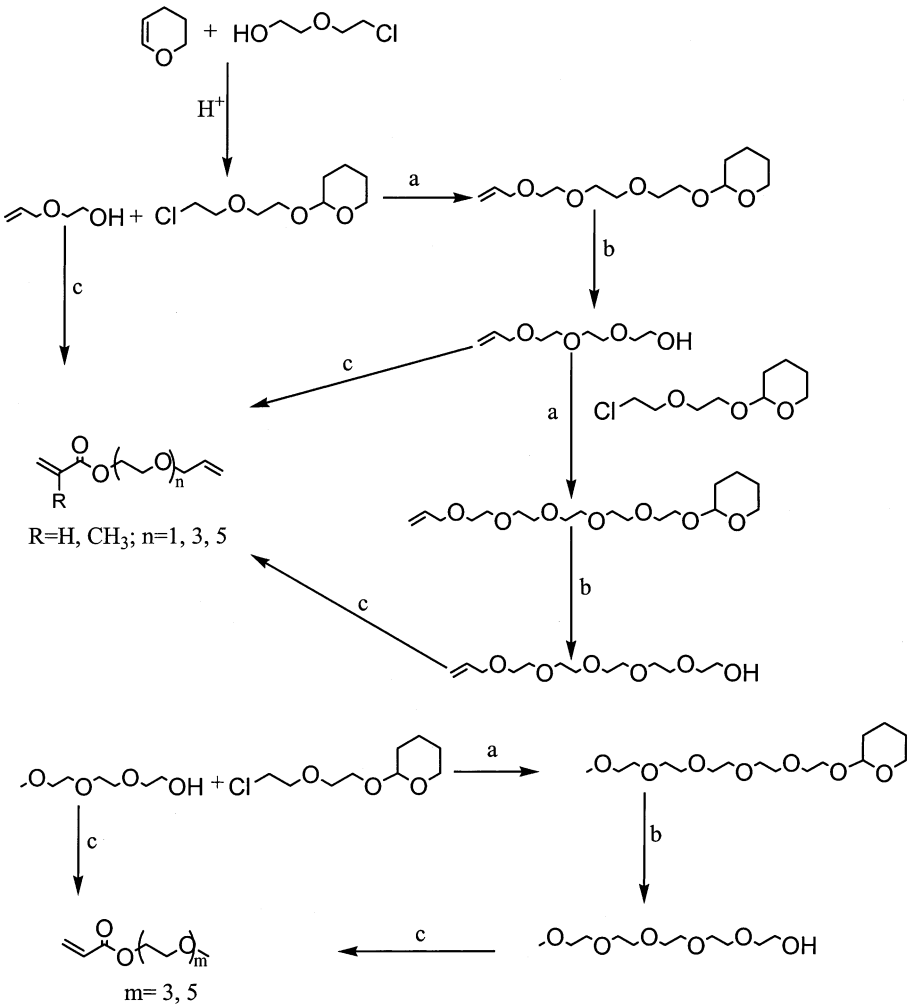

Note: a. 50 wt% $NaOH/H_2O$, tetrabutylammonium hydrogen sulfate, Toluene
b. HCl, Methanol, reflux
c. Acrylic acid/methacrylic acid, H_2SO_4, hydroquinone, benzene, reflux

aqueous solution, washed with distilled water, and dried with anhydrous $MgSO_4$. The solution was filtered and concentrated on a rotary evaporator and distilled with a purity of 99% by GC analysis. ^1H NMR ($CDCl_3$, ppm): 4.91 (s, 1H), 3.86 (t, 3H), 3.76 (t, 3H), 3.67 (t, 3H), 3.58 (t, 3H), 3.49 (t, 3H), 1.35−1.90 (m, 6H). ^{13}C NMR ($CDCl_3$, ppm): 99.25, 71.60, 70.89, 66.91, 62.5, 43.00, 30.82, 25.67, 19.74. Elemental Analysis: found C 51.87, H 8.48; calculated C 51.80, H 8.15.

2-{2-[2-(2-Allyloxyethoxy)ethoxy]ethoxy}tetrahydropyran. 2-Allyoxyethanol (153 g, 1.5 mol), 2-[2-(2-chloroethoxy)ethoxy]-tetrahydropyran (208 g, 1 mol), and tetrabutylammonium hydrogen sulfate (55 g, 0.162 mol) were mixed with 50% sodium hydroxide aqueous solution (400 mL) and toluene (350 mL). The mixture was heated to 70 °C with mechanical stirring for 16 h. After cooling to room temperature the mixture was poured into 200 g of crushed ice and mixed well. The upper organic layer was isolated, and the aqueous layer was extracted with ether (100 mL × 3). The organic layer was then combined and washed with H_2O (75 mL × 2) and dried over $MgSO_4$. The solution was concentrated on a rotary evaporator. The volatiles were removed under vacuum of 0.2 Torr in 130 °C oil. The residual brownish oil (180 g) in the pot was the crude product. Yield: 66%, 90% pure by GC analysis. This crude product was directly used for the next synthesis step.

2-[2-(2-Allyloxyethoxy)ethoxy]ethanol. 180 g of crude product of 2-{2-[2-(2-allyloxyethoxy)ethoxy]ethoxy}tetrahydropyran was dissolved in 300 mL of ethanol, and 10 mL of concentrated HCl in 50 mL of distilled water was added. The solution was refluxed overnight, neutralized with $NaHCO_3$, and concentrated under reduced pressure. The residual oil was vacuum-distilled, and the fraction at 85−87 °C/0.15 T was collected to yield 105 g product; yield: 84%, 98% pure by GC analysis. ^1H NMR ($CDCl_3$, ppm): 5.80 (m, 1H), 5.16 (d, 1H), 5.07 (d, 1H), 3.91 (d, 2H), 3.4−3.7 (m, 12H), 2.80 (s, 1H). ^{13}C NMR ($CDCl_3$, ppm): 134.90, 117.43, 72.77, 72.47, 70.87, 70.81, 70.56, 69.58, 61.89. Elemental Analysis: found C 56.45, H 9.24; calculated C 54.84, H 9.47.

2-[2-(2-{2-[2-(2-Allyloxyethoxy)ethoxy]ethoxy}ethoxy)ethoxy]-tetrahydropyran. The crude product was obtained as described for 2-{2-[2-(2-allyloxyethoxy)ethoxy]ethoxy}tetrahydropyran as a brown oil; yield: 54%, 91% pure by GC analysis. This crude product was directly used for the next synthesis step.

2-(2-{2-[2-(2-Allyloxyethoxy)ethoxy]ethoxy}ethoxy)ethanol. The crude product was obtained as described for 2-[2-(2-allyloxyethoxy)ethoxy]ethanol as a brownish oil. It was then distilled at 0.15 Torr, and the fraction that boiled at 124−126 °C was collected; yield: 82%, 99% pure by GC analysis. ^1H NMR ($CDCl_3$, ppm): 5.87 (m, 1H), 5.24 (d, 1H), 5.15 (d, 1H), 3.99 (d, 2H), 3.5−3.8 (m, 20H), 2.72 (s, 1H). ^{13}C NMR ($CDCl_3$, ppm): 135.01, 117.38, 72.79, 72.49, 70.87, 70.83, 70.59, 69.65, 61.98. Elemental Analysis: found C 55.60, H 9.58; calculated C 56.12, H 9.35.

2-[2-(2-{2-[2-(2-Methoxyethoxy)ethoxy]ethoxy}ethoxy)ethoxy]-tetrahydropyran. Following the same procedure as for 2-{2-

Scheme 2. Synthesis of Prepolymers

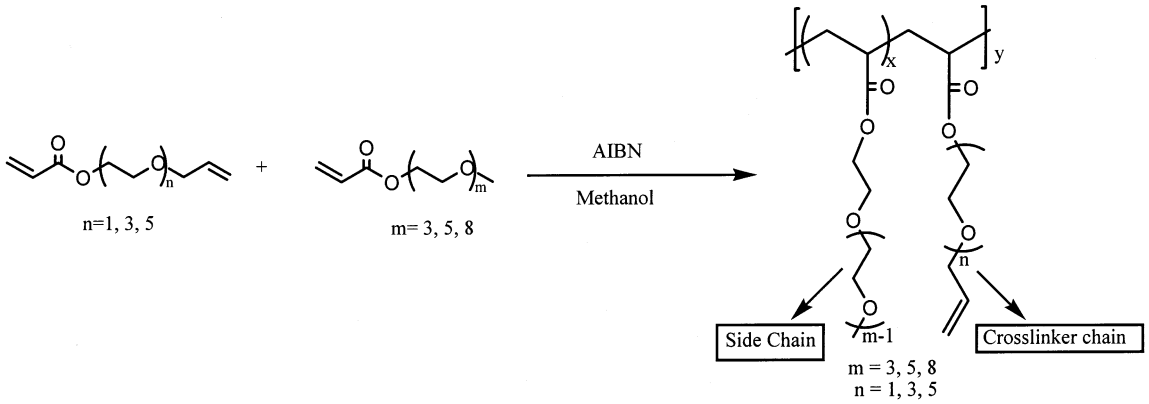

[2-(2-allyloxyethoxy)ethoxy]ethoxy}tetrahydropyran triethylene glycol monomethyl ether (300 g, 1.83 mol), 2-[2-(2-chloroethoxy)ethoxy]tetrahydropyran (208 g, 1 mol), and tetrabutylamonium hydrogen sulfate (55 g, 0.162 mol), 50% sodium hydroxide aqueous solution (400 mL) and toluene (350 mL) were used. After work-up, removal of volatiles by rotary evaporation, and further purification by distillation under high vacuum of 0.2 Torr in a 130 °C oil bath, viscous liquid was left; 200 g, yield 59%, 82.5% pure by GC analysis. This crude product was used directly for the next synthesis step.

2-(2-{2-[2-(2-Methoxyethoxy)ethoxy]ethoxy}ethoxy)ethanol. Following the same procedure used for 2-[2-(2-allyloxyethoxy)-ethoxy]ethanol, 200 g of 2-[2-(2-{2-[2-(2-methoxyethoxy)ethoxy]-ethoxy}ethoxy)ethoxy]tetrahydropyran was hydrolysized. After work-up and distillation, the fraction at 118−120 °C/0.2 Torr was collected, and 110 g of product was obtained; yield 74.6%, 96.7% pure by GC analysis. ^{1}H NMR ($CDCl_3$, ppm): 3.3−3.6 (m, 20H), 3.25 (s, 3H), 3.08 (t, 1H). ^{13}C NMR ($CDCl_3$, ppm): 72.74, 72.03, 70.71, 70.66, 70.60, 70.46, 61.69, 59.12. Elemental Analysis: found C 51.89, H 9.47; calculated C 52.38, H 9.52.

Synthesis of Acrylate or Methacrylate Monomers. Following the reported procedure,[14] monomethyloligoethylene glycols and 1.5-fold excess of acrylic acid or methacrylic acid, hydroquinone inhibitor, and concentrated sulfuric acid catalyst were dissolved in benzene. The solution was heated to reflux, and water was removed by azeotropic distillation. The reaction was continued for 16 h, after which the solution was cooled to room temperature and washed with 5 wt % NaOH aqueous solution until it is basic. The solution was then washed with distilled water until it is neutral. The solution was dried over anhydrous $MgSO_4$ and filtered. The pure product with a purity of 99% was obtained after removing the solvent on a rotary-evaporator.

2-Allyloxyethyl Acrylate. ^{1}H NMR ($CDCl_3$, ppm): 6.44 (d, 1H), 6.13 (d, 1H), 5.90 (d, 1H), 5.80 (d, 1H), 5.26 (d, 1H), 5.17 (d, 1H), 4.30 (t, 2H), 4.02 (d, 2H), 3.66 (t, 2H). ^{13}C NMR ($CDCl_3$, ppm): 166.44, 134.63, 131.29, 128.51, 117.68, 72.39, 68.09, 64.01. Elemental Analysis: found C 59.97, H 7.96; calculated C 61.54, H 7.69.

2-Allyloxyethyl Methacrylate. ^{1}H NMR ($CDCl_3$, ppm): 6.15 (d, 1H), 5.88 (m, 1H), 5.52 (d, 1H), 5.21 (d, 1H), 5.16 (d, 1H), 4.32 (t, 2H), 3.98 (d, 2H), 3.66 (t, 2H), 1.90 (s, 1H). ^{13}C NMR ($CDCl_3$, ppm): 167.63, 136.37, 134.70, 126.01, 117.50, 72.37, 68.11, 64.63, 18.56. Elemental Analysis: found C 63.35, H 8.29; calculated C 63.53, H 8.24.

2-[2-(2-Allyloxyethoxy)ethoxy]ethyl Acrylate. ^{1}H NMR ($CDCl_3$, ppm): 6.43 (d, 1H), 6.12 (d, 1H), 5.90 (m, 1H), 5.80 (d, 1H), 5.21 (d, 1H), 5.16 (d, 1H), 4.29 (t, 2H), 3.99 (d, 2H), 3.5−3.8 (m, 10H). ^{13}C NMR ($CDCl_3$, ppm): 166.42, 134.94, 131.28, 128.51, 117.40, 72.47, 70.90, 70.86, 69.63, 69.35, 63.94. Elemental Analysis: found C 59.02, H 8.20; calculated C 59.98, H 8.01.

2-(2-{2-[2-(2-Allyloxyethoxy)ethoxy]ethoxy}ethoxy)ethyl Acrylate. ^{1}H NMR ($CDCl_3$, ppm): 6.39 (d, 1H), 6.14 (d, 1H), 5.90 (m, 1H), 5.80 (d, 1H), 5.21 (d, 1H), 5.16 (d, 1H), 4.27 (t, 2H), 3.98 (d, 2H), 3.5−3.8 (m, 18H). ^{13}C NMR ($CDCl_3$, ppm): 166.50, 135.00, 131.29, 128.53, 117.38, 72.49, 70.87, 70.83, 69.66, 69.36, 63.96. Elemental Analysis: found C 57.62, H 8.50; calculated C 57.83, H 8.43.

Scheme 3. Synthesis of LiBAMB

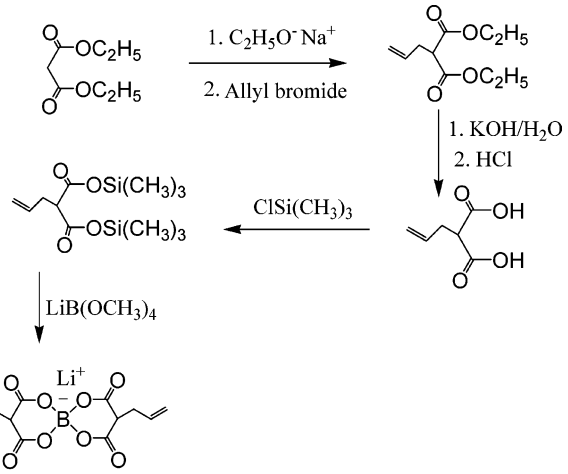

LiBAMB

2-[2-(2-Methoxyethoxy)ethoxy]ethyl Acrylate. ^{1}H NMR ($CDCl_3$, ppm): 6.33 (d, 1H), 6.06 (d, 1H), 5.74 (d, 1H), 4.22 (t, 2H), 3.4−3.8 (m, 10H), 3.29 (s, 3H). ^{13}C NMR ($CDCl_3$, ppm): 166.38, 131.24, 128.49, 72.11, 70.65, 69.31, 63.91, 59.22. Elemental Analysis: found C 53.99, H 8.40; calculated C 55.05, H 8.26.

2-(2-{2-[2-(2-Methoxyethoxy)ethoxy]ethoxy}ethoxy)ethyl Acrylate. ^{1}H NMR ($CDCl_3$, ppm): 6.36 (d, 1H), 6.08 (d, 1H), 5.77 (d, 1H), 4.25 (t, 2H), 3.4−3.8 (m, 18H), 3.31 (s, 3H). ^{13}C NMR ($CDCl_3$, ppm): 166.38, 131.25, 128.51, 72.15, 70.80, 69.33, 66.85, 63.93, 59.26. Elemental Analysis: found C 55.33, H 8.63; calculated C 54.90, H 8.50.

2.3. Synthesis of Prepolymers (Scheme 2). The following is a specific example of the polymerization of 2-[2-(2-methoxyethoxy)ethoxy]ethyl acrylate-*co*-2-allyloxyethyl acrylate to illustrate the general polymerization procedure of acrylates or methacrylates. 2-[2-(2-Methoxyethoxy)ethoxy]ethyl acrylate (21.8 g, 0.1 mol) and 2-allyloxyethyl acrylate (2.46 g, 0.016 mol) were mixed in 250 mL of methanol, and 0.16 g of AIBN (1 mol % relative to double bonds) was added as the initiator. The solution was degassed first and then flushed with dry argon. The above process was repeated three times, and finally the solution was heated to 60 °C for 3 days. The solution was concentrated and precipitated into dry diethyl ether twice. The prepolymer was dried under high vacuum over P_2O_5 for 2 days. 15.5 g of viscous liquid was obtained; yield 61.0%. M_w 5.13 × 10^4 g/mol, PDI = 1.26. ^{1}H NMR ($CDCl_3$, ppm): 5.85 (m, 1H), 5.23 (d, 1H), 5.17 (d, 1H), 4.15 (t, 14H), 3.98 (d, 2H), 3.4−3.8 (m, 66H), 3.34 (s, 19H), 2.30 (t, 7H), 1.63 (d, 14H). ^{13}C NMR ($CDCl_3$, ppm): 174.50, 135.61, 115.54, 72.18, 70.85, 70.78, 69.16, 63.72, 59.28, 36.60, 31.55.

Scheme 4. Synthesis of Network Single Ion Conductors

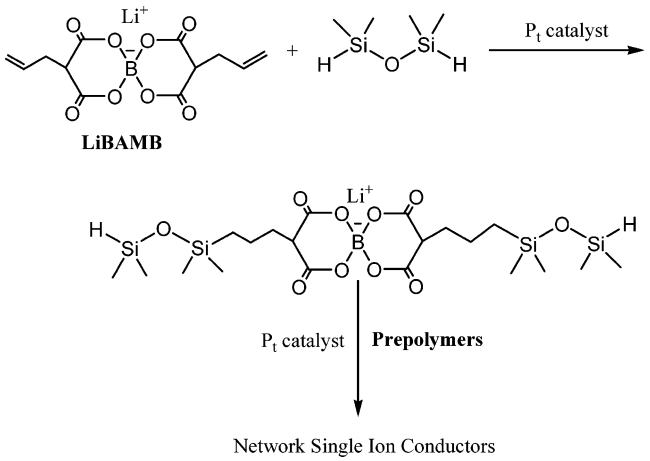

2.4. Synthesis of Salt (Scheme 3). *LiB(OCH$_3$)$_4$* was synthesized according to the literature[15] with a yield of 93.6%. ^{1}H NMR (DMSO-d_6, ppm): 3.16 (s). ^{13}C NMR (DMSO-d_6, δ, ppm): 48.56.

2-Allyldiethyl malonate was synthesized following the literature procedure[16] with a yield of 30%. 92% pure by GC analysis. ^{1}H NMR ($CDCl_3$, ppm): 5.70 (m, 1H), 5.2(d, 1H), 5.17 (d, 1H), 4.14 (q, 4H), 3.42 (t, 1H), 2.61 (t, 2H), 1.29 (t, 6H). ^{13}C NMR ($CDCl_3$, ppm): 169.50, 134.47, 117.60, 61.49, 53.28, 33.23, 14.33.

2-Allylmalonic Acid. To a hot solution of 26 g of KOH in 60 mL of water, 33 g of 2-allyldiethyl malonate was added slowly under vigorous stirring. When the reaction solution became clear, it was cooled and poured carefully into 200 mL of hydrochloric acid solution. The resulting organic solution was extracted with ether (150 mL × 4). The combined ether was dried over $MgSO_4$ and filtered. Ether was removed, and 19.6 g of product was obtained with a yield of 82.5%, 95% by GC analysis. ^{1}H NMR ($CDCl_3$, ppm): 5.78 (m, 1H), 5.16 (d, 1H), 5.10 (d, 1H), 3.51 (t, 1H), 2.68 (t, 2H). ^{13}C NMR ($CDCl_3$, ppm): 169.21, 134.43, 117.51, 53.21, 33.20.

2-Allyldi(trichloromethylsilyl) Malonate (AllylDTMSM). Following the literature procedure,[17] 23 g of 2-allylmalonic acid was mixed with 50 mL of chlorotrimethylsilane and 50 mL of 1,2-dichloroethane. The solution was refluxed in 80 °C oil bath for 4 days. Solvent was removed on a rotary evaporator. The residual was distilled, and the fraction at 73−74 °C/0.25 T was collected. 26 g of product (AllylDTMSM) was obtained; yield: 35%, 96.7% pure by GC analysis. ^{1}H NMR ($CDCl_3$, ppm): 5.79 (m, 1H), 5.03 (d, 1H), 4.97(d, 1H), 3.38 (t, 1H), 2.57 (t, 3H), 0.27 (s, 18H). ^{13}C NMR ($CDCl_3$, ppm): 167.35, 135.90, 117.80, 45.13, 31.10, −0.15.

Lithium Bis(alllylmalonato)borate (LiBAMB). 6.0 g of LiB(OCH$_3$)$_4$ (0.042 mol) and 24.2 g of AllylDTMSM (0.084 mol) were mixed in 200 mL of anhydrous acetonitrile and heated in a 45−50 °C oil bath for 24 h. After the reaction was completed, the solvent was removed by rotary evaporator at 50 °C and by drying in a vacuum oven at 75 °C for 24 h. It is difficult to recrystallize from acetonitrile/benzene solution, so the solid was dissolved in acetonitrile and filtered, the solvent was removed under reduced pressure, and 11.0 g of product was obtained after drying under vacuum at 85 °C for 2 days; yield 86.7%. ^{1}H NMR (DMSO, ppm): 5.75 (m, 1H), 5.02 (d, 1H), 4.98 (d, 1H), 3.54 (t, 1H), 2.56 (t, 2H). ^{13}C NMR (DMSO, ppm): 168.20, 135.90, 117.78, 48.12, 31.16. Elemental Analysis, found C 47.55, H 4.33; calculated C 47.68, H 3.97.

2.5. Synthesis of Network Single Ion Conductors (Scheme 4). *Intermediate I.* Tetramethyldisiloxane (36 g, 0.27 mol) was dissolved in 100 mL of dry THF, and 0.34 g of Pt catalyst was added. The solution was stirred at 70 °C, and 4.0 g of LiBAMB (0.0132 mol) dissolved in 50 mL of THF was added to this solution slowly under the purge of dry N_2. The reaction was continued for 3 days, after which the ^{1}H NMR spectrum showed that double bond signal from LiBAMB had disappeared, indicating the addition reaction was completed. The solvent was removed, and the residual solid was dried in the antechamber of a glovebox; 8.9 g of solid was isolated. ^{1}H NMR ($CDCl_3$, ppm): 4.64 (m, 1H), 3.42 (t, 1H), 1.80 (t, 2H), 1.37 (m, 2H), 0.49 (t, 2H), 0.15 (m, 12H). ^{13}C NMR (DMSO, ppm): 168.90, 48.34, 31.31, 20.90, 18.43, 1.46, 1.25. Elemental Analysis: found C 41.75, H 7.39; calculated C 42.11; H 7.02.

Single Ion Conductors. Equivalent amounts of intermediate I and prepolymers were dissolved in dry THF and refluxed for 5 days under the Pt catalyst.The apparent cross-linking by the lithium salt grafting was observed by the precipitation of the product from the solution. The solvent was removed, and the crude single ion conductors were dried in a vacuum oven at 50 °C overnight, after which they were extracted with dry THF to remove unreacted intermediate I. Finally, the single ion conductors were dried in a vacuum oven at 85 °C over P_2O_5 for 2 days.

2.6. Measurements. ^{1}H and ^{13}C NMR (TMS as internal reference) spectra were collected on a Bruker 300 NMR spectrometer. The GC experiment was performed on a 5890 series II plus gas chromatograph with a SPB5 column (Supelcowax 30 m, 0.32 mm i.d., film thickness 0.25 μm) and carrier gas of helium (3 mL/min) with a temperature program of 5 min at 40 °C, 10 °C/min to 230 °C, and 5 min at 230 °C. Elemental analysis was performed on a Perkin-Elmer series II CHNS/O analyzer 2400.

Glass transition temperatures T_g were measured using a Perkin-Elmer-7 DSC instrument. The heating rate was kept at 10 °C/min. The molecular weights of the prepolymers were determined by using Agilent 1100 series HPLC equipped with a refractive index detector. A PLgel 10 μm miniMIX-B 250 × 4.6 mm column was employed with THF eluent and calibrated by using polystyrene standard samples in THF with molecular weights ranging from 500 to 3 000 000.

The measurement of ac conductivity was carried out using a Swagelok cells that have been described before.[18,19] A Solartron SI 1254 four-channel frequency response analyzer and a 1286 electrochemical interface were used to measure the impedance of the electrolyte films of known thickness in constant volume cells with blocking electrodes. Li/Li cells were constructed inside a helium-filled drybox, and the cell cycling was carried out at 85 °C using an Arbin BT 4020 mutichannel cycler.

3. Results and Discussion

3.1. Preparation of Monomers and Network Single Ion Conductors. The allyl-terminated and methoxy-terminated oligoethylene glycols were synthesized by stepwise chain extension and hydrolysis as shown in Scheme 1. Gas chromatography (GC) was used to monitor the process and the identity of the distilled product was confirmed by ^{1}H NMR. The final terminated glycols were esterified with acrylic acid or methacrylic acid using catalytic amounts of concentrated sulfuric acid rather than with acryloyl chloride or methacryloyl chloride via the catalysis of triethylamine, since the product obtained through the former process is of higher purity, and also the byproduct of triethylamine hydrogen chloride of the latter process is difficult to remove completely.

The prepolymers were obtained by free radical polymerization in methanol at 65 °C with AIBN as the initiator. They were purified by repeated precipitations from methanol into dry ether.

The synthesis of network single ion conductors proceeded through two steps. Intermediate compounds were synthesized by reacting LiBAMB with excess tetramethyldisiloxane, and their identities were confirmed in the ^{1}H NMR spectra through the disappearance of the double bond signal from the salt and the

Table 1. Physical Properties of Prepolymers

prepolymers	R	*m*	*n*	*x*	M_n	M_w	PDI	T_g/°C	appearance
polyacrylates	H	3	1	6.33	4.07×10^4	5.13×10^4	1.26	−56.0	viscous liquid
	H	5	1	7.80	9.32×10^3	1.48×10^4	1.59	−64.7	viscous liquid
	H	5	1	3.80	1.17×10^4	2.20×10^4	1.88	−63.0	viscous liquid
	H	5	1	1.80	1.35×10^4	3.12×10^4	2.31	−59.5	viscous liquid
	H	5	1	0.80	6.58×10^4	1.17×10^5	1.78	−44.8	glassy
	H	8	1	2.27	5.92×10^3	8.25×10^3	1.39	−61.3	viscous liquid
	H	8	1	1.08	9.89×10^6	1.54×10^7	1.56	−55.7	rubber
	H	8	3	0.84	6.93×10^3	8.97×10^3	1.30	−58.7	viscous liquid
	H	8	5	0.60	5.00×10^3	7.86×10^3	1.57	−61.1	viscous liquid
polymethacrylates	CH_3	8	1	1.06	1.77×10^6	2.73×10^6	1.54	−55.9	rubber

presence of a silane signal. The obtained intermediates were then reacted with prepolymers using a platinum catalyst in dry THF. To ensure complete reaction, a higher catalyst concentration and extended reaction time was used. The residual unreacted intermediates were removed from the single ion conductors by extraction with THF, in which the intermediates were well dissolved.

3.2. Physical Properties of Prepolymers and Single Ion Conductors. The obtained polyacrylate or polymethacrylate polymers varied in mechanical properties from viscous liquids to rubbers, depending on the molar ratio of the two monomers used. The general physical properties of these prepolymers are listed in Table 1.

The glass transition temperatures of prepolymers depend on both the ratios of two monomers used and also upon the number of EO units in the two monomers. For the prepolymers from the same starting monomers of pentaethylene glycol monomethyl ether acrylate and allyloxyethyl acrylate, the more allyloxyethyl acrylate that the polymer contained (the smaller value of *x* in Table 1 (see also Scheme 2)) the higher were the molecular weights and glass transition temperatures. At similar molar ratios of the two monomers used for copolymerization, it was observed that the glass transition temperature of the resulting prepolymers was higher with fewer EO units in the side chains of the two monomers. For example, the glass transition temperature of the prepolymer from triethylene glycol monomethyl ether acrylate and alloyoxyethyl acrylate ($x = 6.33$, $T_g = -56$ °C) is higher than that of the prepolymer from pentaethylene glycol monomethyl ether acrylate and allyloxyethyl acrylate ($x = 7.80$, $T_g = -64.7$ °C). This also holds true for the prepolymers from the same monomer of poly(ethylene glycol) monomethyl ether acrylate ($n = 8$) and different comonomers; i.e., the glass transition temperature of the prepolymer from the comonomer of allyloxyethyl acrylate (1 EO unit) ($x = 1.08$, $T_g = -55.7$ °C) is higher than that from the comonomer of 2-[2-(2-allyloxyethoxy)ethoxy]ethyl acrylate (3 EO unit) ($x = 0.84$, $T_g = -58.7$ °C), which is higher than that from the comonomer of 2-(2-{2-[2-(2-allyloxyethoxy)ethoxy]ethoxy}ethoxy)ethyl acrylate (5 EO unit) ($x = 0.60$, $T_g = -61.1$ °C).

After cross-linking with LiBAMB by hydrosilylation, the glass transition temperature of the resulting dry single ion conductor increases with respect to that of the corresponding prepolymer. Here the increase of glass transition temperature is due to not only the cross-linking by the bridging lithium salt but also a result of the complexation of lithium cation by carboxylate groups in the anion and by the oligoether side chains.

3.3. Ionic Conductivity. *Effect of Side Chain Length-PAE_mXE_1-40.* Figure 1 shows the ionic conductivities of network single ion conductors having same cross-linker chain length and different side chains at the same salt concentration of EO/Li = 40. As can be seen from the Figure 1, the conductivity systematically increases with increasing the side chain length. The best ambient temperature conductivity of 1.8×10^{-8} S cm^{-1} is obtained for the single ion conductor with a side chain length of three ethylene oxide (EO) units; it increases to 2.7×10^{-8} S cm^{-1} when side chain length is five EO units and reaches the highest room temperature conductivity of 1.9×10^{-7} S cm^{-1} when side chain length is eight EO units. This is consistent with previously reported conductivities of binary salt (LiTFSI) solutions of polyacrylate ethers where it was observed that the maximum values were obtained with side chains that were at least six EO units long.[20] In general, a difference in ionic conductivity is either caused by a difference in the number of charge carriers or by the ionic mobility. As suggested by Nishimoto et al. in polyether-based network polymer electrolytes with hyperbranched side chains,[21] it is quite unlikely that the dissociation of the lithium salt differs enough to cause the changes in conductivity reported above because the chemical structure of the single ion conductor is so similar. The conductivity difference must be accounted for by the difference of ionic mobility, which is due to the difference in the mobility of the side chains within the network. As reflected in Table 2, the glass transition temperature of the single ion conductor decreases with an increase in the side chain length, which is consistent with an increase in side chain mobility.

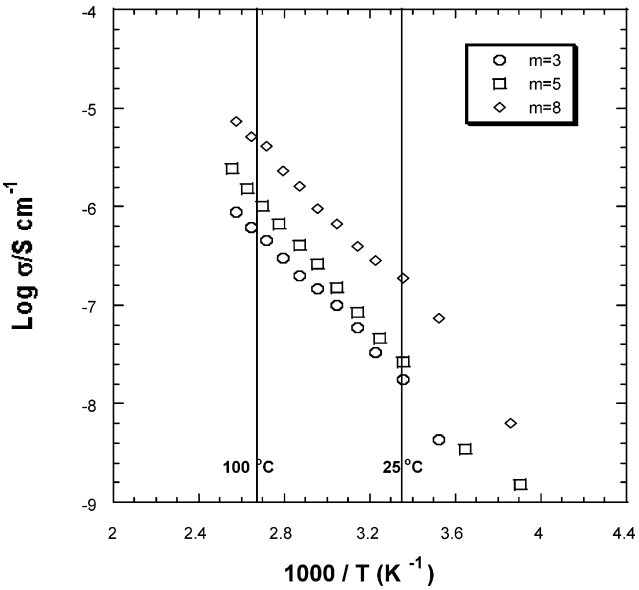

Figure 1. Arrhenius plots of ionic conductivities of single ion conductors with general formula of PAE_mXE_1 (one EO unit in cross-linker and different EO units in the side chains) at the salt concentration of EO/Li = 40.

Table 2. Glass Transition Temperature (T_g) and Ambient Conductivity (log σ) of Single Ion Conductors

polymers	R	*m*	*n*	*x*	EO/Li	polymer code	T_g/°C	log σ/S cm^{-1}
	H	3	1	6.33	40/1	PAE_3XE_1-40	−52.2	−7.75
	H	5	1	7.80	80/1	PAE_5XE_1-80	−55.4	−7.96
	H	5	1	3.80	40/1	PAE_5XE_1-40	−54.7	−7.57
	H	5	1	1.80	20/1	PAE_5XE_1-20	−52.5	−7.94
polyacrylates	H	5	1	0.80	10/1	PAE_5XE_1-10	−37.2	N/A
	H	8	1	2.27	40/1	PAE_8XE_1-40	−56.4	−6.73
	H	8	1	1.08	20/1	PAE_8XE_1-20	−50.4	−7.04
	H	8	3	0.84	20/1	PAE_8XE_3-20	−51.5	−6.76
	H	8	5	0.60	20/1	PAE_8XE_5-20	−53.0	−6.46
polymethacrylates	CH_3	8	1	1.06	20/1	$PMAE_8XE_1$-20	−48.5	−7.34

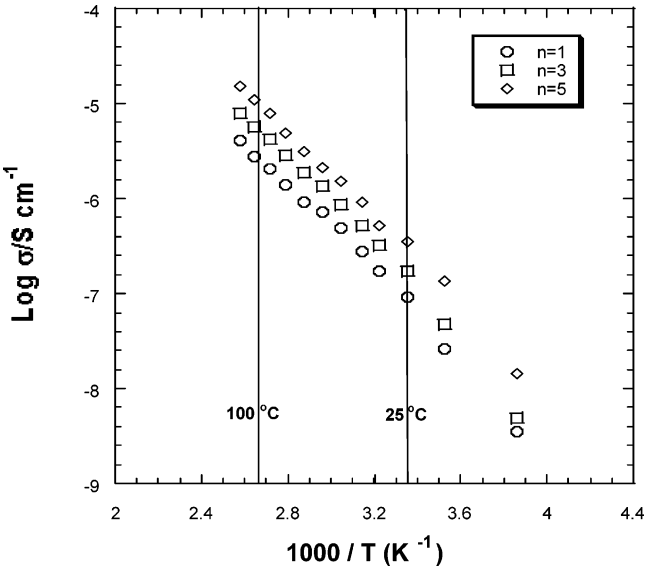

Figure 2. Arrhenius plots of ionic conductivities of single ion conductors with general formaula of PAE_8XE_n (eight EO units in the side chain and different EO units in cross-linker chain) at the same concentration of EO/Li = 20.

Effect of Cross-Linker Chain Length-PAE_8XE_n-20. Figure 2 shows the ionic conductivity of single ion conductors having same side chain and different anion cross-linker chain lengths at the same salt concentration of EO/Li = 20. In this case, the number of EO units in the side chain was kept at eight while the number of EO units in the cross-linker changes. It should be noted that the number of EO units in the cross-linker of the prepolymer is different from that in the cross-linking bridge of the single ion conductor, since each lithium salt, LiBAMB, was connected to two cross-linkers of the prepolymer. Thus, the number of EO units in each bridge of the single ion conductor is double the number of EO units in the prepolymer. The conductivity in Figure 2 showed similar behavior as observed in Figure 1 for the effect of side chain length; i.e., conductivity increases with increasing the cross-linker length. As discussed in the previous paragraph, the main contribution to the ionic conductivity difference is from the ion mobility difference. In these polymers, it is observed that a longer bridge between the polymer main chains will result in a more flexible network and thus a higher ionic mobility. The higher mobility of networks containing longer cross-linkers is confirmed from the lower glass transition temperatures, as shown in Table 2. However, it should also be noted that the effect of cross-linker on conductivity is not as pronounced as that of the side chain. The highest ambient temperature conductivity is 9.1×10^{-8} S cm^{-1} for $n = 1$, 1.7×10^{-7} S cm^{-1} for $n = 3$, and 3.5×10^{-7} S cm^{-1} for $n = 5$.

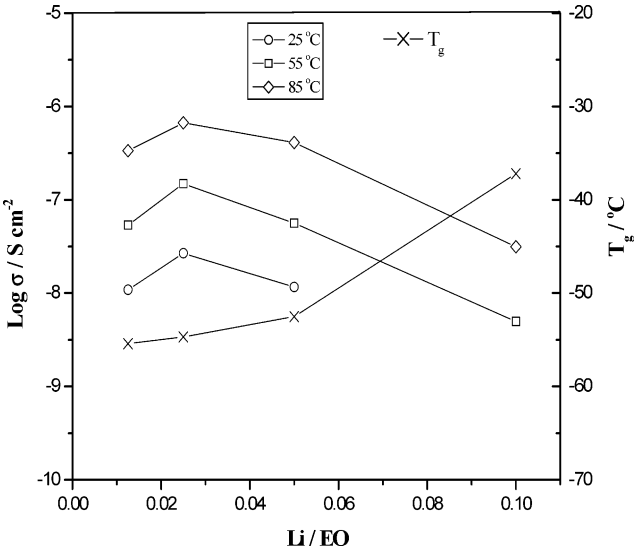

Figure 3. Glass transition temperatures T_g and ionic conductivities for PAE_5XE_1-based network single ion conductors at varying temperatures.

Effect of Salt Concentration-PAE_5XE_1. Figure 3 shows the glass transition temperatures T_g and ionic conductivities for PAE_5XE_1-based network single ion conductors at several temperatures. As observed in conventional solid polymer electrolytes,[22−24] the ionic conductivity initially increases with increasing salt concentration, passes a maximum, and then decreases. The best conductivity was found at EO/Li = 40 with a value of 1.2×10^{-8} S cm^{-1} at 25 °C. In contrast to the ionic conductivity, the glass transition temperature continually increases with increasing salt concentration. The increase of glass transition temperature with salt concentration is not only due to the increase of chemical cross-linking density but also due to the intermolecular and intramolecular coordination of lithium cations, which act as transient physical cross-linking points in the polymer electrolytes. The increase in T_g results in a decrease of segmental motion of the matrix polymer and thus reduces the mobility of free cations; however, the number of free cations increases with increasing salt concentration. The combination of these two opposite effects results in the ionic conductivity maximum observed in Figure 3.[22−24]

Effect of Plasticizer. The conductivities of these new single ion conductors as seen in Figures 1−3 are low, suggesting that the severe ion pairing occurred in these systems. To improve the ionic conductivity, a solvent mixture of EC/DMC (1/1, wt/wt) was added to form gel polyelectrolytes. This particular combination was selected due to its best combination of dielectric constant and viscosity. The gels were only formed from the series of PAE_5XE_1 with different salt concentrations to elucidate the effect of plasticizer. The isothermal ionic

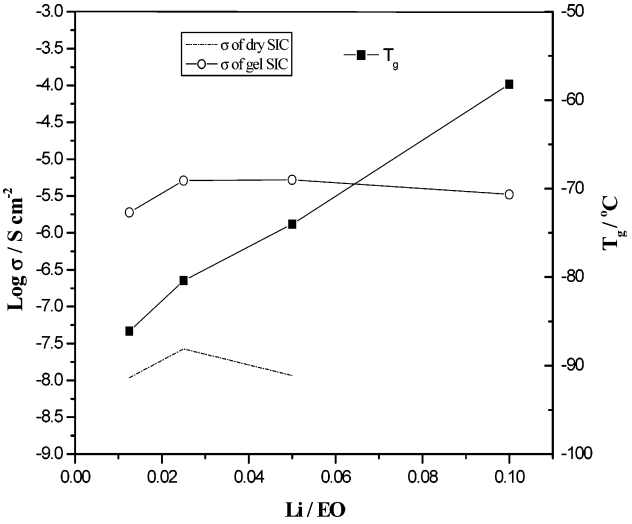

Figure 4. Dependence of ionic conductivity and glass transition temperature on salt concentration for PAE_5XE_1-based gel single ion conductors containing 50 wt % EC/DMC (1/1, wt/wt).

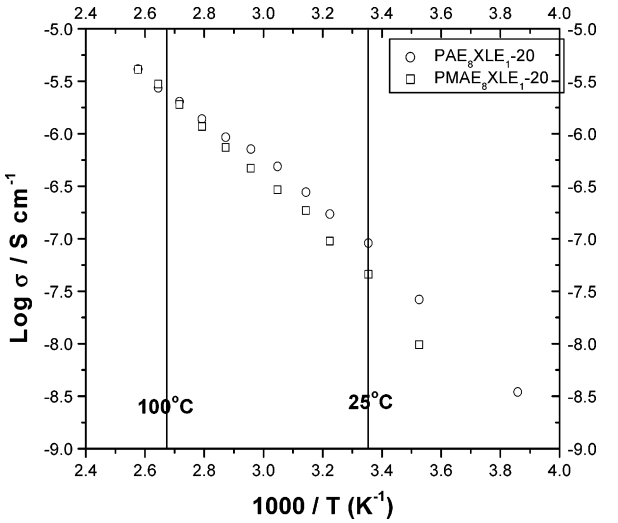

Figure 5. Comparison of ionic conductivity of polyacrylate-based single ion conductor with that of polymethacrylate-based single ion conductor at the same salt concentration of EO/Li = 20.

conductivities of the resulting gel single ion conductors containing 50 wt % of EC/DMC at 25 °C is shown in Figure 4. To facilitate a direct comparison, the conductivities of the dry single ion conductors are also included in the figure as dashed lines. As can be seen in the figure, the conductivities of the gel single ion conductors are 2 orders of magnitude higher than those of the dry single ion conductors across all the salt concentrations. The addition of plasticizer not only increases the ion mobility by providing a microscopically liquid environment but also apparently increases the number of conducting ions through better dissociation in the high dielectric constant media. The highest ambient temperature conductivity of 7.9×10^{-6} S cm^{-1} is obtained for the gel single ion conductor with a salt concentration of EO/Li = 40.

Effect of Polymer Backbone. Figure 5 compares the ionic conductivity of polyacrylate-based single ion conductor with that of polymethacrylate-based single ion conductor at the same salt concentration of EO/Li = 20. At lower temperatures the conductivity of polyacrylate-based single ion conductor is slightly higher than that of polymethyacrylate-based single ion conductor; however, at higher temperatures their conductivities tend to merge. The conductivity difference at lower temperatures is primarily due to the differences in their glass transition temperatures which are listed in Table 2.

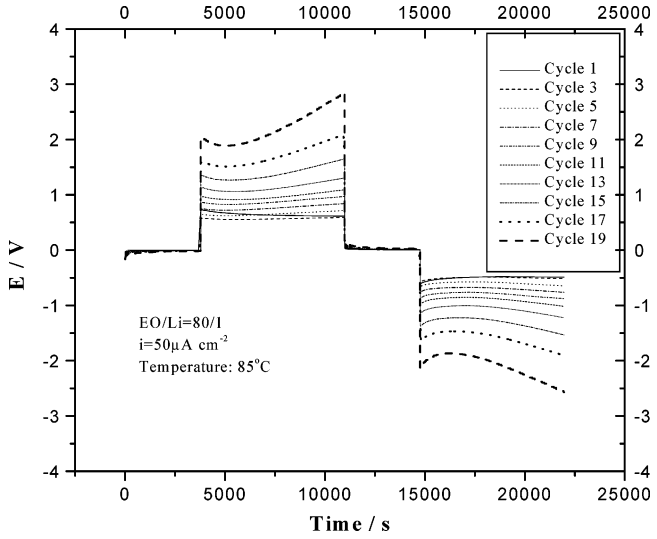

Figure 6. Cycling profile the Li/Li cell of a dry single ion conductor with a salt concentration of EO/Li = 80/1 under the sequence of 1 h relaxation, 2 h charge, 1 h relaxation, and 2 h discharge at a current density of 50 μA cm^{-2}.

3.4. Li/Li Cell Cycling Performance. The dry single ion conductors were used to construct Li/Li cells, which were cycled under the sequence of 1 h relaxation, 2 h charge, 1 h relaxation, and 2 h discharge at different current densities. One typical cycling performance of dry single ion conductor PAE_5XE_1-80 is shown in Figure 6. The cell was cycled at a current density of 50 μA cm^{-2}. Since there are no published reports describing the behavior of single ion conductors between nonblocking lithium electrodes under charge/discharge conditions, there are no direct comparisons to mention here. However, the result shown in Figure 6 has two distinct features, which, we believe, is unique to the behavior of single ion conductors. First of all, for all cycles (except the first cycle) shown in the figure, once the current was turned on, the cell potential immediately increased to a value determined by the ohmic and interfacial impedances and did not increase further with time, which is distinctly different from the behavior of binary salt conductors in which cell potential increases further over time due to the concentration polarization.[25] Second, the behavior of the cell during the very first charge cycle, i.e., the cell potential falls with time, also appears to be a special feature of this network type single ion conductor. The cations were complexed by either the side chains or the cross-linker chains, and the anions were fixed between the polymer chains and cannot move on the time scale of the initial current pulse (due to the low ionic conductivity), which resulted in an initial potential higher than that determined by the combined bulk and interfacial impedance (Figure 7). The polymer chains themselves are not fully extended like the ideal two-dimensional network structure drawn on paper. However, once the current is turned on, the lithium cations move through the membrane by means of the polymer segmental motion, which results in some relaxation of the polymer chains. The anions will also move around due to segmental motion but the range of

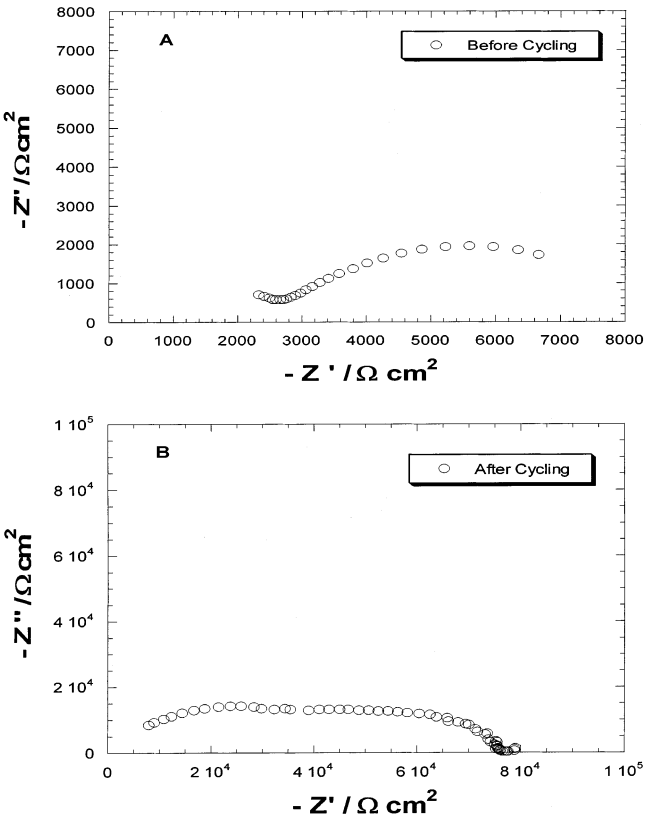

Figure 7. Impedance spectra of the cell from Figure 6 before (A) and after (B) cycling.

motion will be limited by the length of the side chain that tethers them to the polymer backbone. If observed carefully, the final cell potential during the first charge cycle is very close to the calculated cell potential from the combined bulk and interfacial impedances (Figure 7). The decrease of the potential may be due to polymer relaxation processes in the bulk or on the surface but may equally be due to nucleation on the lithium metal electrode. Further experimentation is required to elucidate the sources of the potential variations. The potential increase with continued cycling is apparently related to reactions on the surface of lithium metal, leading to a buildup of the SEI layer and thus the increase of the interfacial impedance. The source of the SEI formation, which was confirmed by the following post mortem analysis result, is from the decomposed small species (organic or inorganic lithium salts). These mobile species were responsible for the potential tail up in the final charge/discharge period as observed after 10 cycles, which is due to concentration polarization.

3.5. Postmortem Analysis. The failed Li/Li cells were disassembled inside a glovebox. The polymer electrolyte was scraped off the electrode, dissolved in a small amount of distilled water, and extracted with dichloromethane. GC was used to analyze the extracted compounds, and a typical chromatogram is shown in Figure 8. The peak with a retention time of 20.355 min is identical to that of the synthesized pure side chain starting material, penta(ethylene glycol) monomethyl ether, which means that the polymers were decomposed from the ester sites of the side chains. Similar results were observed for other single ion conductors with side

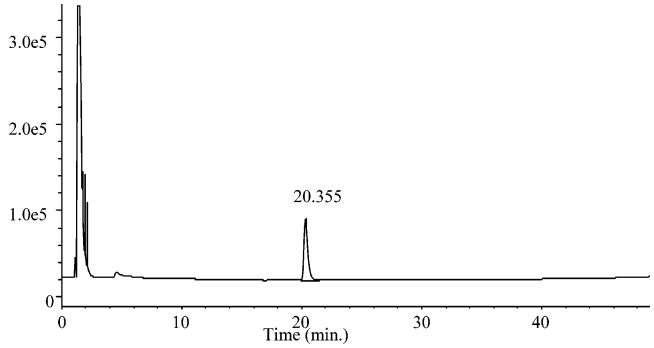

Figure 8. Gas chromatograph (GC) of the extraction of the aqueous solution of failed Li|dry single ion conductor with EO/Li = 80| Li cell with dichloromethane.

chain lengths of three and eight EO units. This GC result is consistent with the observed increases in both cell potential and interfacial impedance in Figures 6 and 7, respectively, which appear to be mainly due to the decomposition of the comb branches at the ester sites.

The result shown in Figure 8 suggests that the ester group is not stable against the lithium metal under charge/discharge conditions. In addition, the conductivity of these dry single ion conductors is too low for practical applications. To improve ionic conductivity, different polymers need to be synthesized. Usually polyepoxides have lower glass transition temperatures than those of polyacrylates, so higher mobility of ions is expected. In addition, the ether bond of polyepoxide is less easily reduced than the ester bond of polyacrylate and should be more stable against the lithium metal when cycled under charge/discharge condition. Through the same variation scheme shown for polyacrylate-based single ion conductors, the conductivity of polyepoxide-based single ion conductors can also be optimized.[26] The results of the optimization of ionic conductivity and cell performance of polyepoxide-based single ion conductors will be reported in a separate paper.[27]

4. Conclusions

Polyacrylate/polymethacrylate-based network single ion conductors containing the LiBAMB salt have been successfully synthesized and tested as electrolytes for rechargeable lithium batteries. An increase in the number of ethylene oxide units in both the side chain and the cross-linker chain leads to an increase in the ionic conductivity of new single ion conductors. An optimum in conductivity is observed for salt concentration that results from the increase in charge carriers vs the increase in T_g with salt concentration. Plasticizer increases the ionic conductivity of gel single ion conductor by more than 2 orders of magnitude relative to that of the dry single ion conductor. The Li/Li cycling performance of dry single ion conductor showed no polarization, and nearly no relaxation was observed. An increase of cell potential with cycling is caused by the increase of the interfacial impedance arising from the formation of a SEI layer. The main reason for cell failure appears to be due to the decomposition of the ester group in the side chains.

Acknowledgment. This work was financially supported by the NASA PERS program (NASA Glenn).

References and Notes

(1) Gray, F. M., Ed.; *Solid Polymer Electrolytes: Fundamentals and Technological Applications*; VCH Publishing: New York, 1991.
(2) (a) Mehta, M. A.; Fujinami, T.; Inoue, T. *J. Power Sources* **1999**, *81*−*82*, 724. (b) Mehta, M. A.; Fujinami, T.; Inoue, S.; Matushita, K.; Inoue, T. *Electrochim. Acta* **1999**, *45*, 1175.
(3) (a) Sun, X. G.; Angell, C. A. *Electrochim. Acta* **2001**, *46*, 1467. (b). Sun, X. G.; Xu, W.; Zhang, S. S.; Angell, C. A. *J. Phys.: Condens. Matter* **2001**, *13*, 8235. (c) Xu, W.; Sun, X. G.; Angell, C. A. *Electrochim. Acta* **2003**, *48*, 2255.
(4) Ito, Y.; Ohno, H. *Solid State Ionics* **1995**, *79*, 300.
(5) Zhou, G. B.; Khon, I. M.; Smid, J. *Polym. Commun.* **1989**, *30*, 52.
(6) Kobayashi, N.; Uchiyama, M.; Tsuchida, E. *Solid State Ionics* **1985**, *17*, 307.
(7) Tsuchida, E.; Shigehara, K. *Mol. Cryst. Liq. Cryst.* **1984**, *106*, 361.
(8) Benrabah, D.; Sylla, S.; Alloin, F.; Sanchez, J. Y.; Armand, M. *Electrochim. Acta* **1995**, *40*, 2259.
(9) Onishi, K.; Matsumoto, M.; Nakacho, M.; Shigehara, K. *Chem. Mater.* **1996**, *8*, 469.
(10) Fujinami, T.; Tokimune, A.; Mehta, M. A.; Shriver, D. F.; Rawsky, G. C. *Chem. Mater.* **1997**, *9*, 2236.
(11) Xu, W.; Angell, C. A. *Solid State Ionics* **2002**, *147*, 295.
(12) Sun, X. G.; Angell, C. A. *Solid State Ionics*, in press.
(13) Xu, W.; Angell, C. A. *Electrochem. Solid-State Lett.* **2001**, *4*, E1.
(14) Sun, X. G.; Lin, Y. Q.; Jing, X. B. *Solid State Ionics* **1996**, *83*, 79.
(15) Barthel, L.; Buestrich, R.; Carl, E.; Gores, H. J**.** *J. Electrochem. Soc.* **1996**, *143*, 3572.
(16) Legoff, E.; Ulrich, S. E.; Denney, D. B. *J. Am. Chem. Soc.* **1958**, *80*, 622.
(17) Hergott, H. H.; Simchen, G. *Synthesis* **1980**, 626.
(18) Ma, Y. P.; Doyle, M.; Fuller, T. F.; Doeff, M. M.; De Jonghe, L. C.; Newman, J. *J. Electrochem. Soc.* **1995**, *142*, 1859.
(19) Doeff, M. M.; Edman, L.; Sloop, S. E.; Kerr, J. B.; De Jonghe, L. C. *J. Power Sources* **2000**, *89*, 227.
(20) Buriez, O.; Han, Y. B.; Hou, J.; Kerr, J. B.; Qiao, J.; Sloop, S. E.; Tian, M.; Wang, S. *J. Power Sources* **2000**, *89*, 149.
(21) Nishimoto, A.; Agehara, K.; Furuya, N.; Watanabe, T.; Watanabe, M. *Macromolecules* **1999**, *32*, 1541.
(22) Kobayashi, N.; Uchiyama, M.; Shigehara, K.; Tsuchida, E. *J. Phys. Chem.* **1985**, *89*, 987.
(23) Tsuchida, E.; Kobayashi, N.; Ohno, H. *Macromolecues* **1988**, *21*, 96.
(24) Synder, J. E.; Ratner, M. A.; Shriver, D. F. *J. Electrochem. Soc.* **2003**, *150*, A1090.
(25) Kerr, J. B.; Sloop, S. E.; Liu, G.; Han, Y. B.; Hou, J.; Wang, S. *J. Power Sources* **2002**, *110*, 389.
(26) Marchese, L.; Andrei, M.; Roggero, A.; Passerini, S.; Prosperi, P.; Scrosati, B. *Electrochim. Acta* **1992**, *37*, 1559.
(27) Sun, X. G.; Craig, R.; Liu, G.; Han, Y. B.; Kerr, J. B. *J. Am. Chem. Soc.*, in preparation.

MA035690G